Frequency-Tunable Multigigawatt Sub-Half-Cycle Light Pulses from Coupled-State Dynamics of Optical Solitons and Impulsively Driven Molecular Vibrations

A. M. Zheltikov,[1] A. A. Voronin,[1] R. Kienberger,[2,3] F. Krausz,[2,4] and G. Korn[2]

[1]*Physics Department, International Laser Center, M. V. Lomonosov Moscow State University, Vorob'evy gory, Moscow 119992, Russia*
[2]*Max-Planck-Institut für Quantenoptik, Hans-Kopfermann-Strasse 1, D-85748 Garching, Germany*
[3]*Fakultät für Physik, Technische Universität München, James Franck Straße, 85748 Garching, Germany*
[4]*Department für Physik, Ludwig-Maximilians-Universität, Am Coulombwall 1, D-85748 Garching, Germany*

(Received 15 January 2010; published 30 August 2010)

Coupling ultrashort optical field waveforms to ultrafast molecular vibrations in an impulsively excited Raman medium is shown to enable the generation of frequency-tunable sub-half-cycle multigigawatt light pulses. In a gas-filled hollow waveguide, this coupled-state dynamics is strongly assisted by soliton effects, which help to suppress temporal stretching of subcycle optical pulses, providing efficient Raman-type impulsive excitation of ultrafast molecular vibrations over large propagation paths.

DOI: 10.1103/PhysRevLett.105.103901 PACS numbers: 42.65.Tg, 42.65.Re

Advanced laser sources capable of generating few-cycle light pulses [1] provide unique tools to detect, understand, and control the fastest atomic motions in molecular systems [2] and enable direct time-domain studies of attosecond electron dynamics in the gas- and condensed-phase media [3]. The scaling of such laser sources to higher levels of field intensities and the extension of ultrafast science approaches to complex real-life, many-body systems with many degrees of freedom call for the development of efficient and practical techniques for the nonlinear-optical spectral transformation of few-cycle light pulses. Here, we demonstrate that coupling ultrashort field waveforms to a molecular coherence of an impulsively excited Raman medium can enable the generation of frequency-tunable sub-half-cycle multigigawatt light pulses. The Raman effect in gas-phase materials has been earlier shown to allow a synthesis of few- and single-cycle field waveforms [4–8]. The Raman-type optical nonlinearity of silica fibers, on the other hand, has long been known to give rise to a continuous redshift of the carrier frequency of a soliton [9]. Intrapulse Raman scattering in capillary-type [10–12] and photonic-crystal [13,14] hollow waveguides has been shown to induce a redshift of high-power light pulses, offering interesting options for the frequency conversion of ultrashort pulses and all-optical pump-seed synchronization in optical parametric chirped-pulse amplification of few-cycle field waveforms [15,16]. Below in this Letter, we show that, in a gas-filled hollow waveguide with carefully managed dispersion, nonlinearity, attenuation, and ionization, soliton effects can enhance coupling between subcycle optical field waveforms and ultrafast molecular vibrations by suppressing temporal stretching of optical pulses. As a result of this coupled-state dynamics, frequency-tunable multigigawatt sub-half-cycle light pulses can be generated in an anomalously dispersive hollow waveguide without additional pulse compression.

When a high-peak-power ultrashort laser pulse interacts with a molecular system, driving fast vibrations in this system and experiencing modulation through a backreaction of molecules to the light field, phenomenological models of the nonlinear-optical response of a molecular system, which characterize nonlinear-optical processes in terms of field-independent material constants, often become inadequate. Here, we analyze the evolution of ultrashort optical field waveforms in an extended Raman-active medium by solving an appropriate, slowly-evolving-wave-approximation-type [17,18] modification of the generalized nonlinear Schrödinger equation [9] for the evolution of the optical field [Eq. (S1) of supplementary material, Ref. [19]]. This equation is solved jointly with the equation for the electron-density dynamics due to photoionization [Eq. (S2) in Ref. [19]] and optical Bloch equations [Eqs. (S3), (S4) in Ref. [19]] for the amplitudes of molecular vibrations and rotations driven by the laser pulse and the population differences for the relevant vibrational and rotational transitions.

For efficient spectral transformation of light pulses whose pulse widths are on the order of the field cycle T_0, we choose to work with hydrogen molecules, which provide the shortest vibration time (vibration period $\tau_v = 2\pi/\Omega_v \approx 8$ fs, where Ω_v is the molecular vibration frequency) among all the immediately available molecular systems. For molecular hydrogen, we take the nonlinear refractive index $n_2 \approx 5 \times 10^{-19}(p/p_0)$ $\mathrm{W^{-1}\,cm^2}$ (p is the gas pressure, p_0 is the atmospheric pressure), vibrational (v) and rotational (r) population relaxation times $T_{1v,r} \approx$ 1 ns, coherence relaxation times $T_{2v} \approx 200$ ps and $T_{2r} \approx$ 100 ps, $\Omega_v/2\pi \approx 125$ THz, rotational frequency $\Omega_r/2\pi \approx$ 17.6 THz, and vibrational and rotational molecular polarizabilities $\kappa_v \approx 4.9 \times 10^{-41}\,\mathrm{C\,m^2/V}$ and $\kappa_r \approx 1.6 \times 10^{-41}\,\mathrm{C\,m^2/V}$. Dispersion of molecular hydrogen is defined as $n_{\mathrm{H}}(\omega) = 1 + 0.5(p/p_0)[S_1(\omega_1^2 - \omega^2)^{-1} + S_2(\omega_2^2 - \omega^2)^{-1}]$, where $S_1 = 0.0725\,\mathrm{fs^{-2}}$, $S_2 = 0.0595\,\mathrm{fs^{-2}}$, $\omega_1 = 20\ \mathrm{fs^{-1}}$, $\omega_2 = 25.7\ \mathrm{fs^{-1}}$. The photoionization rate is calculated by using the Keldysh model [20] with the ionization potential $U_i = 15.43$ eV and the initial density of

neutral species $\rho_0 = 2.7 \times 10^{19}(p/p_0)$ cm^{-3}. Waveguide dispersion and loss are calculated by solving the dispersion equation for the fundamental mode of the gas-filled hollow waveguide. The propagation equation [Eq. (S1) in Ref. [19]] was solved numerically by using the split-step Fourier method with an adaptive mesh. The numerical solution of differential equations (S3) and (S4) in Ref. [19] was based on the fifth-order Runge-Kutta method.

The initial conditions of our simulations are chosen in the form of a Gaussian light pulse $I(t) = I_0 \exp(-t^2/\tau_p^2)$. The spectrum of the input pulse [the dashed line in Fig. 1(a)] is centered at 800 nm and corresponds to a transform-limited pulse width $\tau_p \approx 2.1$ fs (the FWHM pulse width is 3.5 fs). The inner diameter of the hollow waveguide is set equal to 200 μm. The pressure of molecular hydrogen inside the fiber is $p = 0.05$ atm. The entire spectrum of the input laser field then falls within the range of anomalous dispersion [Fig. 1(a)]. The laser spectrum is broad enough to coherently excite vibrational modes of hydrogen molecules ($\Omega_v/(2\pi c) \approx 4155$ cm^{-1}) and H_2^+ molecular ions ($\Omega_v'(2\pi c) \approx 2170$ cm^{-1}, $\tau_v' = 2\pi/\Omega_v' \approx 15.4$ fs). However, according to our calculations using the Keldysh-type formalism [20], the density of H_2^+ ions never exceeds 10^{14} cm^{-3} within the range of laser intensities and gas pressures considered here. The relevant molecular polarizability of H_2^+ ions is estimated [21] as $\kappa_v' \approx 1.2 \times 10^{-41}$ C m^2/V. The contribution of vibrational modes of H_2^+ ions to the overall coherent response of the gas is thus a factor of 5×10^4 lower than the contribution of vibrational modes of hydrogen molecules.

The coupled-state dynamics of ultrashort light pulses and molecular coherence is illustrated in Figs. 2(a)–2(d), which map the spectral, as well as spatiotemporal evolution of the light field and molecular coherence in a hollow waveguide optimized for efficient wavelength shifting of ultrashort light pulses. To provide efficient impulsive, Raman-type excitation of molecular vibrations, light pulses need to be shorter than the period of molecular vibrations τ_v, with the pulse-width optimum defined as [12] $\tau_{\rm opt} \approx (2\ln 2)^{1/2}\pi^{-1}\tau_v$. A pulse with such a short pulse width can strongly drive molecular rotations and vibrations in the gas filling the waveguide, thus providing a strong coupling between the optical field and molecular motions. As a part of this coupled-state dynamics, the optical field is scattered off the Raman coherence, experiencing a continuous redshift [Fig. 2(a)] as it propagates down the waveguide.

In the linear regime of pulse propagation (for low laser peak powers), dispersion tends to stretch ultrashort light pulses [dash-dotted line in the inset of Fig. 1(b)], weakening the coupling between the optical field and molecular modes. To suppress dispersion-induced pulse stretching, we work in the parameter space where the anomalous waveguide dispersion supports the solitonic propagation of ultrashort light pulses. In this regime, the balance between the nonlinear and dispersion-induced phase shifts keeps light pulses short [Fig. 2(b)] even for propagation paths exceeding the dispersion length $l_d = \tau_p^2|\partial^2\beta/\partial\omega^2|_{\omega_0}^{-1}$, which is estimated as 35 cm for the above-specified conditions. This type of pulse evolution scenario is crucial for the efficient frequency conversion of single-cycle pulses as it helps to maintain strong coupling between the optical field and molecular vibrations over large propagation paths inside a waveguide. In Fig. 2(e), we illustrate the soliton-compression phase of pulse evolution by presenting the results of simulations where the Raman part of nonlinearity has been switched off. Here, the light pulse is compressed from 2.1 fs at the input of the waveguide to about 1 fs at $z = 20$ cm [Fig. 2(e)]. The optimal soliton-compression length l_c can be estimated by using a simple empirical formula obtained as the best fit for the numerical solution of the nonlinear Schrödinger equation [9], $l_c \approx [C_1(N)^{-1} + C_2(N)^{-2}]\xi_0$, where $C_1 \approx 0.32$,

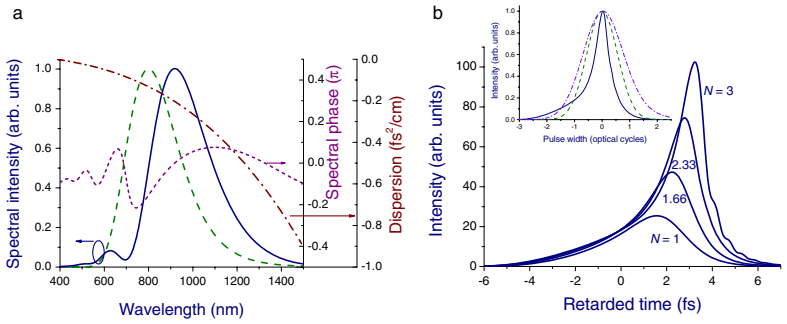

FIG. 1 (color online). (a) The spectrum (solid line) and the spectral phase profile (dotted line) of an ultrashort laser pulse transmitted through a hollow waveguide filled with molecular hydrogen. The spectrum of the input pulse is shown by the dashed line. The dash-dotted line presents the wavelength dependence of group-velocity dispersion for the fundamental waveguide mode of the gas-filled hollow waveguide. The input pulse energy is 80 μJ; the waveguide length is 30 cm. (b) Intensity envelopes for laser pulses transmitted through 25 cm of the hollow waveguide for different soliton numbers N, as indicated next to the curves. (Inset) Temporal envelopes of the input laser pulse (dashed line) and the laser pulse transmitted through 30 cm of the hollow waveguide for the input pulse energy of 1 μJ (dash-dotted line) and 80 μJ (solid line). For all the plots, the input pulse width is 2.1 fs, the inner diameter of the hollow waveguide is 200 μm, and the pressure of molecular hydrogen inside the waveguide is 0.05 atm.

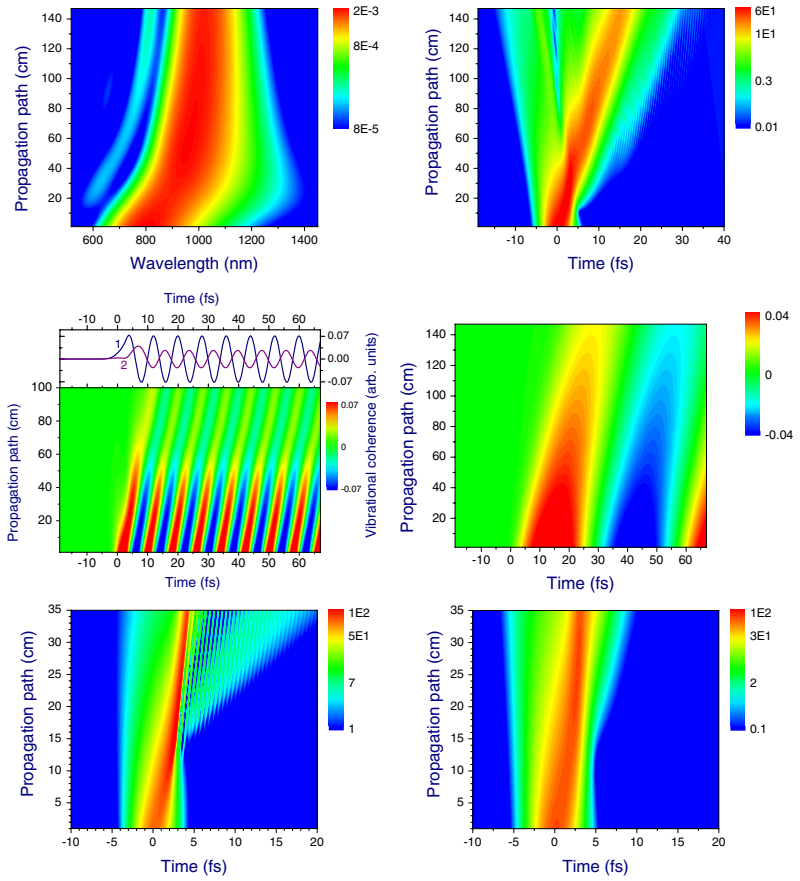

FIG. 2 (color online). Coupled-state dynamics of a single-cycle soliton and molecular coherence: (a) spectral intensity of the light field as a function of the wavelength and propagation path, (b) field intensity, (c) vibrational, and (d) rotational parts of molecular coherence as functions of the propagation path and retarded time. (e),(f) Dynamics of the light pulse within the initial section of the waveguide (e) with Raman effect switched off and (f) in the presence of the Raman effect. The upper panel of Fig. 2(c) shows temporal cross sections of the vibrational coherence at $z =$ 20 cm (1) and 60 cm (2). The input pulse width is 2.1 fs, the input pulse energy is 80 μJ, the inner diameter of the hollow waveguide is 200 μm, and the pressure of molecular hydrogen inside the waveguide is 0.05 atm.

$C_2 \approx 1.1$, $N = [l_d^{(2)}/l_{\mathrm{nl}}]^{1/2}$ is the soliton number, and $\xi_0 = \pi l_d^{(2)}/2$ is the spatial period of the fundamental soliton. This estimate yields $l_c \approx 20$ cm for the soliton dynamics considered here, which agrees reasonably well with the spatial scale of pulse compression observed in our simulations without the Raman effect [Fig. 2(e)].

The Raman effect redshifts the central wavelength of the soliton pulse, thus inducing additional pulse stretching [cf. Figs. 2(e) and 2(f)]. However, even in the presence of the Raman effect, the soliton pulse compression remains a significant factor at the initial stage of pulse evolution, helping to maintain a short pulse width, thus assisting efficient excitation of molecular vibrations [cf. Figs. 2(b)–2(d)]. Impulsively driven molecular vibrations, in their turn, induce a strong redshift of the light pulse [Fig. 2(a)]. As can be seen from Fig. 2(a), the central frequency of a light pulse with an input pulse width of 2.1 fs is shifted from 800 to 970 nm within a 50-cm propagation path inside the H_2-filled waveguide, where molecular vibrations dominate the Raman response of the molecular gas [see Fig. 2(c)]. With an input pulse energy fixed at 80 μJ, the central wavelength of the output pulse is tuned from 805 to 985 nm by increasing the waveguide length from 1 to 150 cm [Fig. 2(a)]. A waveguide with a fixed length of 150 cm, on the other hand, generates an output whose central wavelength can be tuned from 830 to 990 nm by changing the input pulse energy from 16 to 90 μJ.

Beyond the buildup length of the fundamental soliton, $z > \xi_0 = \pi l_d/2 \approx 55$ cm in Figs. 2(a)–2(d), the group delay between the redshifting soliton and the nonsolitonic part of the field tends to isolate the soliton pulse in the time and frequency domains [Fig. 2(b)]. The soliton pulse exhibits soliton spectral narrowing [Fig. 2(a)] as its central wavelength is shifted to longer wavelengths, where $|\partial^2\beta/\partial\omega^2|$ is larger. As the soliton pulse width becomes much longer than τ_v, strong coupling between the optical field and molecular vibrations can no longer be maintained, and the amplitude of molecular vibrations rapidly falls off [Fig. 2(c)]. Within the propagation path 130 cm $> z >$ 55 cm, a limited soliton redshift can still be achieved as a result of coupling of the optical field with molecular rotations [Figs. 2(a) and 2(d)]. The rate of the frequency shift, however, rapidly decreases as the pulse becomes longer propagating further on along the waveguide [Figs. 2(a) and 2(b)].

For higher input energies, other physical effects, such as ionization and, most importantly, shock-wave formation, enhanced by extremely short pulse widths, can come into play, suppressing the redshift of the laser pulse. Shock-wave features are already noticeable in Figs. 2(e) and 2(f), which visualize the self-steepening of the trailing edge of the pulse within the shock-wave buildup length $l_s \approx 0.4\tau_p\omega_0 l_{\mathrm{nl}} \approx 14$ cm [$l_{\mathrm{nl}} = c(\omega n_2 I)^{-1}$ is the nonlinear length)]. Optimal conditions for the wavelength conversion

of single-cycle light pulses in an anomalously dispersive gas-filled hollow waveguide are thus achieved within the range of input soliton numbers $1.5 < N < 2.5$. Such a choice of input pulse parameters helps to avoid dramatic pulse distortions by shock waves, enabling the generation of wavelength-tunable subcycle light pulses.

In the inset to Fig. 1(b), we illustrate temporal compression of an ultrashort Gaussian laser pulse with $\tau_p = 2.1$ fs, a central wavelength of 800 nm, and a pulse energy of 80 μJ with the use of a 30-cm-long, 200-μm-inner-diameter hollow waveguide filled with molecular hydrogen at $p = 0.05$ atm. The solid line in the inset to Fig. 1(b) shows the temporal envelope of the pulse transmitted through the waveguide. The spectrum of this pulse [the solid line in Fig. 1(a)] is centered at 920 nm and is broad enough to support compression to a transform-limited pulse width of $0.43T_0$ (here the pulse width is defined, similar to a Gaussian pulse width τ_p, as a half-width at the $1/e$ level). The pulse arising in the waveguide as a part of the coupled-state solitonic dynamics is, however, slightly chirped. Its pulse width is 1.35 fs, which corresponds to $0.44T_0$ at 920 nm. The peak power of this sub-half-cycle soliton transient is about 20 GW.

For a more accurate characterization of compressed pulses, we define the time-bandwidth product (TBP) $\xi = \Delta\omega\Delta\tau$, where $(\Delta\omega)^2 = \int_{-\infty}^{\infty}(\omega - \omega')^2|\tilde{A}(\omega, z)|^2 d\omega[\int_{-\infty}^{\infty}|\tilde{A}(\omega, z)|^2 d\omega]^{-1}$ and $(\Delta\tau)^2 = \int_{-\infty}^{\infty}(\theta - \theta')^2|A(\theta, z)|^2 d\theta[\int_{-\infty}^{\infty}|A(\theta, z)|^2 d\theta]^{-1}$, where $\omega' = \int_{-\infty}^{\infty}\omega|\tilde{A}(\omega, z)|^2 d\omega[\int_{-\infty}^{\infty}|\tilde{A}(\omega, z)|^2 d\omega]^{-1}$ and $\theta' = \int_{-\infty}^{\infty}\theta|A(\theta, z)|^2 d\theta[\int_{-\infty}^{\infty}|A(\theta, z)|^2 d\theta]^{-1}$. The transform-limited TBP, calculated as a product of the bandwidth of the waveguide output spectrum in Fig. 1(a) and its Fourier transform assuming an ideally flat phase of the waveguide output, is $\xi_0 \approx 0.83$. The TBP for the waveguide output spectrum as shown in Fig. 1(a) and the pulse shape of the same field [inset to Fig. 1(b)] calculated with no flat-phase assumption is $\xi \approx 0.94$. The deviation of the waveguide output from its transform-limited counterpart supported by the output spectrum is due to phase distortions induced by the shock wave, causing the spectral phase of the waveguide output [dotted line in Fig. 1(a)] to deviate from the flat phase profile, needed for the compression to the transform-limited pulse width.

The feasibility of the subcycle-pulse generation strategy demonstrated in this Letter is verified by the robustness of the soliton pulse compression scenario illustrated by Figs. 2(a) and 2(b) with respect to small variations in the parameters of the gas-filled waveguide and input laser pulses. Numerical analysis based on Eqs. (S1)–(S4) of Ref. [19] shows that a 10% decrease in the input pulse energy will reduce the wavelength shift of a soliton at $z = 150$ cm in Figs. 2(a) and 2(b) by approximately 1% and will decrease its energy by 5%, increasing its pulse width by less than 1%. A 10% lengthening of the input pulse, on the other hand, will reduce the wavelength shift of the same soliton by 0.7%, increasing its pulse width by approximately 2%. Finally, a 10% increase in the gas pressure inside the waveguide will increase the soliton wavelength shift by 0.3% and lengthen the compressed soliton pulse by approximately 0.6%.

We have demonstrated that soliton effects in an anomalously dispersive gas-filled hollow waveguide can enhance coupling between subcycle optical field waveforms and ultrafast molecular vibrations. Frequency-tunable multigigawatt sub-half-cycle light pulses can be generated as a transient stage of this coupled-state solitonic dynamics. Intrinsic timing between the wavelength-shifted single-cycle pulse at the output of the waveguide with an ultrashort input pulse suggests an attractive strategy for pump-seed synchronization in optical parametric amplification of extremely short high-peak-power light pulses.

This work was partially supported by the Russian Federal Science and Technology Program (Contracts No. 1130 and No. 02.740.11.0223) and the Russian Foundation for Basic Research (Projects No. 10-02-90051, No. 09-02-12359, and No. 09-02-12373).

[1] E. Goulielmakis *et al.*, Science **317**, 769 (2007).
[2] J. Itatani *et al.*, Nature (London) **432**, 867 (2004).
[3] P. B. Corkum and F. Krausz, Nature Phys. **3**, 381 (2007).
[4] G. Korn, O. Dühr, and A. Nazarkin, Phys. Rev. Lett. **81**, 1215 (1998).
[5] M. Wittmann, A. Nazarkin, and G. Korn, Phys. Rev. Lett. **84**, 5508 (2000).
[6] S. E. Harris and A. V. Sokolov, Phys. Rev. Lett. **81**, 2894 (1998).
[7] A. V. Sokolov *et al.*, Phys. Rev. Lett. **85**, 562 (2000).
[8] N. Zhavoronkov and G. Korn, Phys. Rev. Lett. **88**, 203901 (2002).
[9] G. P. Agrawal, *Nonlinear Fiber Optics* (Academic Press, San Diego, 2001).
[10] J. Herrmann and A. Nazarkin, Opt. Lett. **19**, 2065 (1994).
[11] V. P. Kalosha and J. Herrmann, Phys. Rev. Lett. **85**, 1226 (2000).
[12] V. P. Kalosha and J. Herrmann, Phys. Rev. A **68**, 023812 (2003);
[13] D. G. Ouzounov *et al.*, Science **301**, 1702 (2003).
[14] A. A. Ivanov, A. A. Podshivalov, and A. M. Zheltikov, Opt. Lett. **31**, 3318 (2006).
[15] C. Teisset *et al.*, Opt. Express **13**, 6550 (2005).
[16] E. E. Serebryannikov *et al.*, Phys. Rev. E **72**, 056603 (2005).
[17] R. Bonifacio, R. M. Caloi, and C. Maroli, Opt. Commun. **101**, 185 (1993).
[18] T. Brabec and F. Krausz, Phys. Rev. Lett. **78**, 3282 (1997).
[19] See supplementary material at http://link.aps.org/supplemental/10.1103/PhysRevLett.105.103901 for details of the model.
[20] L. V. Keldysh, Zh. Eksp. Teor. Fiz. **47**, 1945 (1964) [Sov. Phys. JETP **20**, 1307 (1965)].
[21] C.-Y. Hsu, H. J. Lin, and S.-Y. Wang, Chem. Phys. Lett. **145**, 374 (1988).